communications biology

Article

https://doi.org/10.1038/s42003-024-07285-0

miR-276 and miR-182013-5p modulate insect metamorphosis and reproduction via dually regulating juvenile hormone acid methyltransferase

Check for updates

Jiasheng Song[1,2], Wanwan Li[1,2], Lulu Gao[1], Qiang Yan[1], Xinyan Zhang[1], Mingzhi Liu[1] & Shutang Zhou[1]

Juvenile hormone (JH) represses insect metamorphosis and stimulates reproduction. JH titers are generally low in juveniles, drop to a nadir during metamorphosis, increase after eclosion and peak in vitellogenic phase. We found that Jhamt, a rate-limiting enzyme in JH biosynthesis, mirrors JH titer patterns in the migratory locust. Knocking down *Jhamt* reduced JH titers, led to precocious nymphal ecdysis, metamorphosis and impaired vitellogenesis. *Jhamt* is negatively regulated by miR-276 and positively by miR-182013-5p. miR-276 is abundant in late nymphal but low in adults, while miR-182013-5p shows the opposite pattern. In nymphs, miR-276 binds more to *Jhamt*, while in adults, miR-182013-5p dominates. Functionally, miR-276 reduced Jhamt and JH levels, shortening nymphal development and inhibiting Vg expression. Conversely, miR-182013-5p increased Jhamt and JH levels, prolonging nymphal development and enhancing Vg expression. Our findings identify miR-276 and miR-182013-5p as dual regulators in JH biosynthesis, acting as "brake" and "accelerator," respectively. This study provides new insights into JH titer fluctuations and miRNA regulation in insect metamorphosis and reproduction.

Juvenile hormone (JH), an arthropod-specific sesquiterpenoid secreted by corpora allata (CA), plays a pivotal role in insect development, metamorphosis and reproduction[1–3]. In juvenile stage, JH acts as an anti-metamorphic hormone in maintaining the larval/nymphal status by repressing 20-hydroxyecdysone (20E)-induced larva-pupa-adult or nymph-adult transition[2,4]. In adult stage, JH functions as a gonadotrophic hormone in stimulating aspects of reproduction including previtellogenic development, vitellogenesis and egg production (Raikhel et al.[5]; Roy et al.[3]). In many insects, JH titers decline at the onset of pre-metamorphic larval/nymphal molting, and drops to extremely low level or becomes undetectable at metamorphosis[4,6,7]. However, after metamorphosis, JH titers rapidly increase to high levels in previtellogenic adults and reach a peak in vitellogenic stage[5,8–12]. The JH biosynthetic pathway can be divided into two metabolic parts. The early part includes mevalonate pathway to the formation of farnesyl diphosphate (FPP) and is conserved in vertebrates and invertebrates. In the later part, FPP is catalyzed to farnesol and followed by epoxidation or methyl esterification to produce active form of JH, which is specific to insects and other arthropods[13–15]. JH acid methyltransferase (Jhamt), first cloned from silkworm *Bombyx mori* is the rate-limiting enzyme that transfers a methyl group from S-adenosyl-L-methionine to the carboxyl group of either farnesoic acid or JH acid at the final step of JH biosynthesis pathway in insect CA[15–17]. The transcription of *Jhamt* is well correlated the JH production in CA, exerting its vital roles in metamorphosis, vitellogenesis and egg production[2,13,17–20].

Previous studies indicated that, *Jhamt* is regulated at the transcriptional level. During the metamorphosis of fruit fly *Drosophila melanogaster*, the transcription of *Jhamt* was suppressed by 20E receptor complex comprising ecdysone receptor (EcR) and ultraspiracle (USP)[21]. Moreover, Mothers against Dpp (Mad) transduces the activation of Decapentaplegic (Dpp) signals that promote *Jhamt* expression and prevent preconscious metamorphosis in *D. melanogaster*[22]. During the molting and metamorphosis of cricket *Gryllus bimaculatus*, Myoglianin (Myo) acts as a suppressor while Dpp and Glass-bottom boat/60A (Gbb) function as activators for *Jhamt* expression[23]. In *B. mori*, Sex combs reduced (Scr) and POU-M2 bind to *Jhamt* promoter of *Jhamt* and stimulate its expression[24,25]. Although previous studies illustrated the transcriptional regulation of *Jhamt* during

[1]State Key Laboratory of Cotton Bio-breeding and Integrated Utilization, School of Life Sciences, Henan University, Kaifeng, China. [2]These authors contributed equally: Jiasheng Song, Wanwan Li. e-mail: szhou@henu.edu.cn

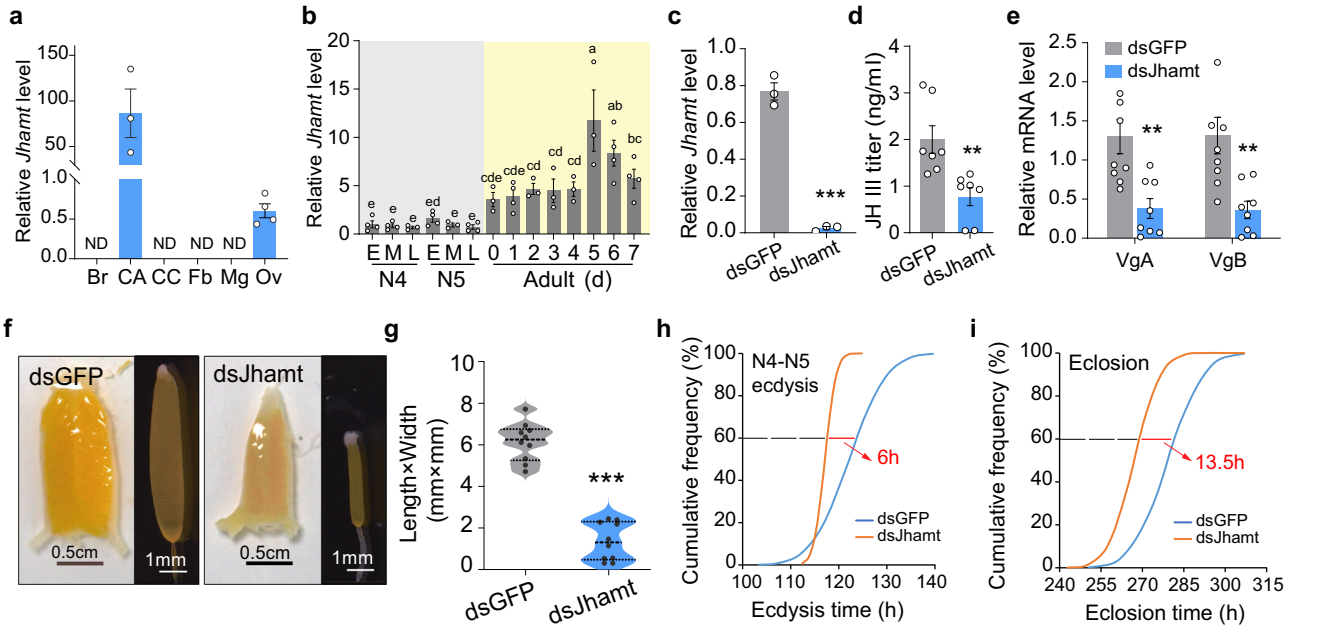

Fig. 1 | Regulation of *Jhamt* in locust metamorphosis and female reproduction. **a** Spatial expression pattern of *Jhamt* in selected tissues. Br brain, CA corpora allata, CC corpus cardiacum, Fb fat body, Mg midgut, Ov ovary, ND nondetectable. Different letters indicate significant differences at $P < 0.05$. $n = 3$. **b** Development expression pattern of *Jhamt* in the CA of penultimate 4th (N4) and final 5th (N5) instar nymphs. E, M, and L indicate the early (day 1), middle (day 2 for N4, and day 3 for N5) and late (day 4 for N4, and day 5 for N5) stages, respectively. $n = 3$–4. **c** RNAi efficiency of *Jhamt* in CA. $^{*}P < 0.05$. $n = 3$. **d** Hemolymph JH titers in adult females treated with dsJhamt vs. dsGFP. $^{**}P < 0.01$. $n = 7$. **e** Effect of *Jhamt* knockdown on *VgA* and *VgB* expression in the fat body. $^{**}P < 0.01$. $n = 8$. **f** Representative phenotypes of ovaries and primary oocytes of adult females treated with dsJhamt vs. dsGFP. **g** Statistical analysis of primary oocyte size after *Jhamt* RNAi. $^{**}P < 0.001$. $n = 10$. **h**, **i** Effect of *Jhamt* RNAi on the ecdysis of 4th and 5th instar nymphs.

metamorphosis, the post transcriptional regulation of *Jhamt* and its regulation in the gonadotrophic development are remains largely unknown.

The endogenous non-coding miRNA, with a length approximately 22-nucleotide, is well known for its post-transcriptional regulatory roles[26]. miRNAs are involved in various aspects such as sex determination, embryogenesis, molting, metamorphosis, reproduction, detoxification and drug resistance[27–31]. A study in *D. melanogaster* illustrated that *Jhamt* is the target of miRNA bantam, misexpression of bantam result in JH-related defects during metamorphosis[32]. In addition, in *Anopheles gambiae* and *Tribolium castaneum*, miR-278, let-7, miR-92b and miR-252 are proved to target *Jhamt* of according to in silico miRNA target prediction and dual-luciferase assay, however the in vivo functions of these miRNAs are still remained undetermined[32]. In addition to directly targeting *Jhamt*, miR-8 has been shown to directly promote cell growth in the CA, leading to increased *Jhamt* levels and elevated JH titers in *D. melanogaster*[33] Thus far, studies on miRNA functions in insect JH synthesis have primarily focused on *D. melanogaster*. Notably, the integrated functions of different miRNAs in regulating *Jhamt* and JH synthesis remain less explored. miR-276 is an evolutionary conserved miRNA in insects with an identical mature sequence of miR-276 in *D. melanogaster*. In *D. melanogaster*, miR-276 is induced by ecdysone and controls the growth through targeting the insulin-like receptor[34]. In *Locusta migratoria*, miR-276 promote the egg-hatching synchrony by upregulating *brahma* (*brm*) in the ovary of locusts[35]. miR-276 (or miR-276 in *D. melanogaster*) also have functions in the nervous system regulating circadian rhythms[36], olfactory[37] and dendrite development[38]. However, its functions in insect JH synthesis remains unclear.

Locusta migratoria has been widely used as a model for studying the mechanisms of JH-dependent female reproduction, as JH controls vitellogenin (Vg) synthesis in the fat body, secretion into the hemolymph, and its uptake by maturing oocytes. Using *L. migratoria* as a model, we have previously demonstrated that two miRNAs let-7 and miR-278 are highly expressed to scavenge JH early response gene *Krüppel-homolog 1* (*Kr-h1*) during nymph-adult transition and downregulated to maintain a high level of *Kr-h1* when vitellogenesis are in progress[39]. Our recent study has identified 17 miRNAs that jointly bind to JH biosynthesis genes and express synchronously at low level during the vitellogenic stage, thereby facilitating JH production[40]. However, the regulatory mechanisms of miRNAs, particularly concerning the rate-limiting enzyme gene *Jhamt*, remain poorly understood. Here we identified that *Jhamt* was negatively regulated by the evolutionarily conserved miR-276 and positively regulated by species-specific miR-182013-5p of locusts. Mechanically, the negative regulator expressed in an opposite manner compared with its target *Jhamt*, while the expression profile of positive regulator miR-182013 mirrors the expression of *Jhamt*. Besides for the distinct expression profile, we further demonstrated that less miR-182013-5p was bond to *Jhamt* than miR-276 in nymphal stage, but more miR-182013-5p was enriched from *Jhamt* mRNA than miR-276 in vitellogenic phase. Our data illustrated that the "braker" miR-276 and "accelerator" miR-182013-5p dually regulate *Jhamt* expression and modulate JH biosynthesis. This study providing a comprehensive perspective on how miRNAs are involved in the precise control of JH titer fluctuations.

Result

Jhamt regulates locust metamorphosis and female reproduction via influencing JH biosynthesis

To identify the functions of *Jhamt*, we preliminary determined its spatial-temporal expression patterns by qRT-PCR. The results showed that *Jhamt* was exclusively expressed in corpora allata (CA) (Fig. 1a). Temporally, *Jhamt* sharply increased by 4.8 times on the day of adult emergence compared to that in the late stage of 5th instar nymph (N5) and maintained a steady level until the 4th day post adult eclosion (PAE). On the 5th day PAE, *Jhamt* rose again, reaching its peak, followed by a gradual decline on the 6th and 7th days PAE (Fig. 1b). To elucidate the functions of *Jhamt*, dsRNA of *Jhamt* was injected into nymph and adult locusts respectively. In the female adults, *Jhamt* was significantly declined by 97% in dsJhamt injected locusts compared with dsGFP treated samples (Fig. 1c). As a result, the amount of JH III in hemolymph in *Jhamt*-depleted locusts was less than a half of those injected with dsGFP (Fig. 1d). Consistent with the decline of JH titer, mRNA levels of *VgA* and *VgB* reduced by 66.4% and 70.1%, respectively in the fat

body (Fig. 1e). Morphologically, *Jhamt*-depleted adult females had blocked oocyte maturation and arrested ovarian growth (Fig. 1f). Statistically, the average length × width index of primary oocyte size was significantly decreased by 74.7% after *Jhamt* knockdown (Fig. 1g). To explore the functions of Jhamt in nymphal locusts, dsJhamt was injected from 4th instar nymph. The results of qRT-PCR showed that *Jhamt* were significantly reduced by 51.2% compared with locusts injected with negative controls (Supplementary Fig. 1a). We found that *Jhamt* depleted locusts molted earlier than those of control groups. Statistically, 60% locusts molted 6 h earlier than the locusts treated with dsGFP (Fig. 1h). And at the time of adult eclosion, a 13.5h-delay for 60% locusts was observed in *Jhamt*-depleted locusts compared to control groups (Fig. 1i). Collectively, these results showed that *Jhamt* is required for JH production. Depletion of *Jhamt* shortened the nymphal stage and retarded oocyte maturation.

Jhamt is downregulated by miR-276 and upregulated by miR-182013-5p

To explore the functions of miRNA in regulating *Jhamt* and JH biosynthesis, we firstly performed target prediction for evolutionary conserved miRNAs. Four miRNAs miR-210, miR-252, miR-282 and miR-276 were predicted to potentially bind to *Jhamt* (Supplementary Fig. 1b, c). To validate the binding sites of miR-210, miR-252, miR-282 and miR-276 on *Jhamt*, we carried out dual-luciferase reporter assays by co-transfection of miRNA mimics and recombinant pmirGLO vectors containing predicted miRNA-binding sites into HEK293T cells. When miR-210, miR-252, miR-282 and miR-276 mimics were co-transfected with pmirGLO vectors respectively, only miR-276 exhibited a significantly effect on reducing the luciferase activity compared with the non-mimic controls (Fig. 2a). As shown in Fig. 2b, the inhibition capacity of miR-276 on relative luciferase activity was completely reversed when the seed sequences were mutated (Fig. 2b and Supplementary Fig. 1c). Notably, according to the miRNA transcriptome data, miR-276 was abundant in CA compared with miR-210, miR-252 and miR-282 (Supplementary Fig. 1d). The spatial expression pattern determined by qRT-PCR showed that miR-276 ubiquitously expressed in Br, CA, CC, Fb, Mg and Ov (Supplementary Fig. 1e). The results above indicating that miR-276 might play a role in regulating *Jhamt* level.

To fully elucidate the regulation of JH synthesis by miRNAs in the CA, linear specific miRNAs were also analyzed besides for the conserved miRNA. We chose 13 locusts-specific miRNAs with the FPKM value bigger than 200 in CA for the preliminary identification. Intriguingly, we found that miR-182013-5p is specifically expressed in CA compared with that in Br, CA, CC, Fb, Mg and Ov (Fig. 2c), indicating a CA-specific role of miR-182013-5p. To clarify whether miR-182013-5p is a canonical miRNA, we quantified the expression level of miR-182013-5p in *Dicer-1* depleted CA. As shown in Fig. 2d, *Dicer-1* levels dropped to 42.2% of the dsGFP injected controls. In the meanwhile, RNA levels of miR-182013-5p and miR-276 in CA significantly reduced by 59.4% and 48.6% (Fig. 2e). We concluded that miR-182013-5p is a Dicer-1 cleaved miRNA similar with other conserved miRNAs as miR-276. To document the functions CA-specific miR-182013-5p, we predicted its target genes in CA. Strikingly, we found that *Jhamt* was the only target predicted by miRanda, microTar and PITA (Supplementary Fig. 1c). To validate the binding site of miR-182013-5p, we carried out dual-luciferase reporter assays using HEK293T cells transfected with recombinant pmirGLO vectors containing 814-bp CDS or 377-bp 3'UTR. When miR-5p-183013 mimics were co-transfected into HEK293T with pmirGLO/*Jhamt*-CDS, luciferase activities declined by 52.3%, compared with the

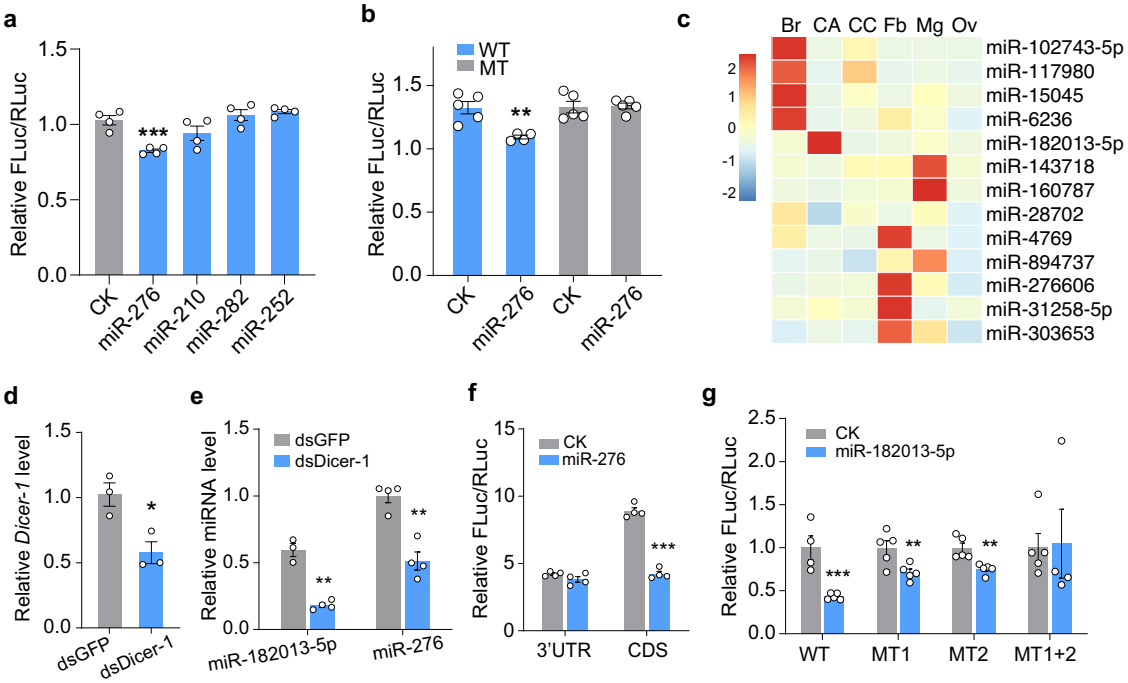

Fig. 2 | Identification of miRNAs targeting *Jhamt*. **a** Dual-luciferase reporter assays using HEK293 cells co-transfected with respective mimics of miR-276, miR-210, miR-282 and miR-252 plus recombinant pmirGLO vectors containing predicted binding sites of *Jhamt*. CK, miRNA mimics. $^{***}P < 0.001$. $n = 4$. **b** Dual-luciferase reporter assays using HEK293 cells co-transfected with miR-276 mimic and recombinant pmirGLO vectors containing predicted binding site (WT) or mutated binding sites (MT) of *Jhamt*. CK, miRNA mimics. $^{**}P < 0.01$. $n = 4$–5. **c** Spatial expression patterns of species-specific miRNAs in locusts. Br brain, CA corpora allata, CC corpus cardiacum, Fb fat body, Mg midgut, Ov ovary. **d** RNAi efficiency of *Dicer-1* in CA. $^{*}P < 0.05$. $n = 3$. **e** Effect of *Dicer-1* knockdown on the expression of miR-182013-5p and miR-276. $^{**}P < 0.01$. $n = 3$–4. **f** Dual-luciferase reporter assays using HEK293 cells co-transfected with miR-182013-5p mimics or miRNA mimics (CK) plus recombinant pmirGLO vectors containing *Jhamt* CDS or 3′UTR sequences. $^{***}P < 0.001$. $n = 4$. **g** Dual-luciferase reporter assays using HEK293 cells co-transfected with miR-182013-5p mimics or miRNA mimics (CK) plus pmirGLO vectors containing wild-type (WT) or mutant (MT) binding sites of *Jhamt*. MT1, mutation of the first miRNA biding site; MT2, mutation of the second binding site; MT1 + 2, mutation in both miRNA-binding sites. $^{**}P < 0.01$. $n = 4$–5. Mann–Whitney *U* test (two-tailed) was applied for comparisons of cells co-transfected with miR-182013-5p mimics *v.s* miRNA mimics plus vectors containing mutations in both miRNA-binding sites (MT1 + 2), as shown in (**g**).

controls (Fig. 2f). However, in cells co-transfected with pmirGLO/*Jhamt*-3'UTR, luciferase activities did not change compared with the cells co-transfected with negative control (ck) (Fig. 2f). As shown in Supplementary Fig. 1c, two binding sites were predicted on CDS region of *Jhamt*. To further verify the binding of miR-182013-5p, seed regions of binding sites was mutated to the complementary sequences. The results showed that individually mutate binding site 1 (MT1) or 2 (MT2) did not fully rescue the inhibition of luciferase activity (Fig. 2g). However, when the two binding sites were both mutated (MT1 + 2), the luciferase activity did not change compared with those co-transfected with mimics of negative control (ck) (Fig. 2f). The results above indicated that miR-182013-5p bind to the CDS of *Jhamt* to regulate its expression. Taken together, *Jhamt* was the potential target of conserved miRNA miR-276 and the locust-specific miRNA miR-182013-5p.

Fluorescence in situ hybridization (FISH) was engaged to identify the co-localization of *Jhamt* with miR-276 or miR-182013-5p. As illustrated in Fig. 3a, miR-276 and miR-182013-5p colocalized with *Jhamt*, respectively, in the cytoplasm of CA cells. To explore the regulatory roles of miR-276 and miR-182013-5p on *Jhamt* in vivo, we overexpressed these two miRNAs by agomiR and decrease their RNA level via antagomiR in adult females (Supplementary Fig. 2a, b). For miR-276, injection of the agomiR result in a decline of *Jhamt* by 40.7% compared with that treated with negative controls (Fig. 3b). While treatment of miR-276 antagomiR leads to the significantly increase of *Jhamt* RNA level (Fig. 3b). The correspond western blot and quantification of band intensity confirmed that protein levels of Jhamt in agomiR-treated locust was declined to 66.4% compared with its normal levels, and injection of miR-276 agomiR resulted in the elevation of protein level by 2.3-fold (Fig. 2c, d). Intriguingly, distinct from the canonical inhibition effects of miR-276 on *Jhamt*, we found that miR-182013-5p has a positive regulatory effect. In detail, injection of miR-182013-5p agomiR increased the RNA level of *Jhamt* by 41.3%, and treatment by miR-182013-5p antagomiR decreased *Jhamt* by 62.8% (Fig. 3e). Western blot and subsequent quantification of band intensity showed that Jhamt protein levels in CA was increased by 1.3-fold and decrease by 36.7% (Fig. 3f, g). To further validate the in vivo regulations of miR-276 and miR-182013-5p on *Jhamt*, we examined the *Jhamt* RNA abundant in nymph stage after agomiR and antagomiR treatment. Consistent with the results in female adults, decrease of miR-276 leads to a significant increase of *Jhamt*, while overexpression of miR-276 played an opposite effect on *Jhamt* level (Supplementary Fig. 2c, d). miR-182013-5p also positively regulate *Jhamt* in the nymph stage (Supplementary Fig. 2e, f). These results collectively illustrated that miR-276 and miR-182013-5p play opposite regulatory roles on *Jhamt* in vivo.

miR-276 attenuates JH biosynthesis for locust metamorphosis and reproduction

In order to explore the functions of miR-276 and miR-182013-5p, antagomiR was utilized for knocking down the miRNA level in vivo. After injection of miR-276 antagomiR in the female adult, the relative JH titer significantly increased by 4.2-fold compared with control (Fig. 4a). As a result, *VgA* and *VgB* mRNA levels elevated by 1.7-fold and 1.5-fold in fat body, respectively (Fig. 4b). Western blot in the fat body and band intensity quantification demonstrated that injection of miR-276 antagomiR caused a

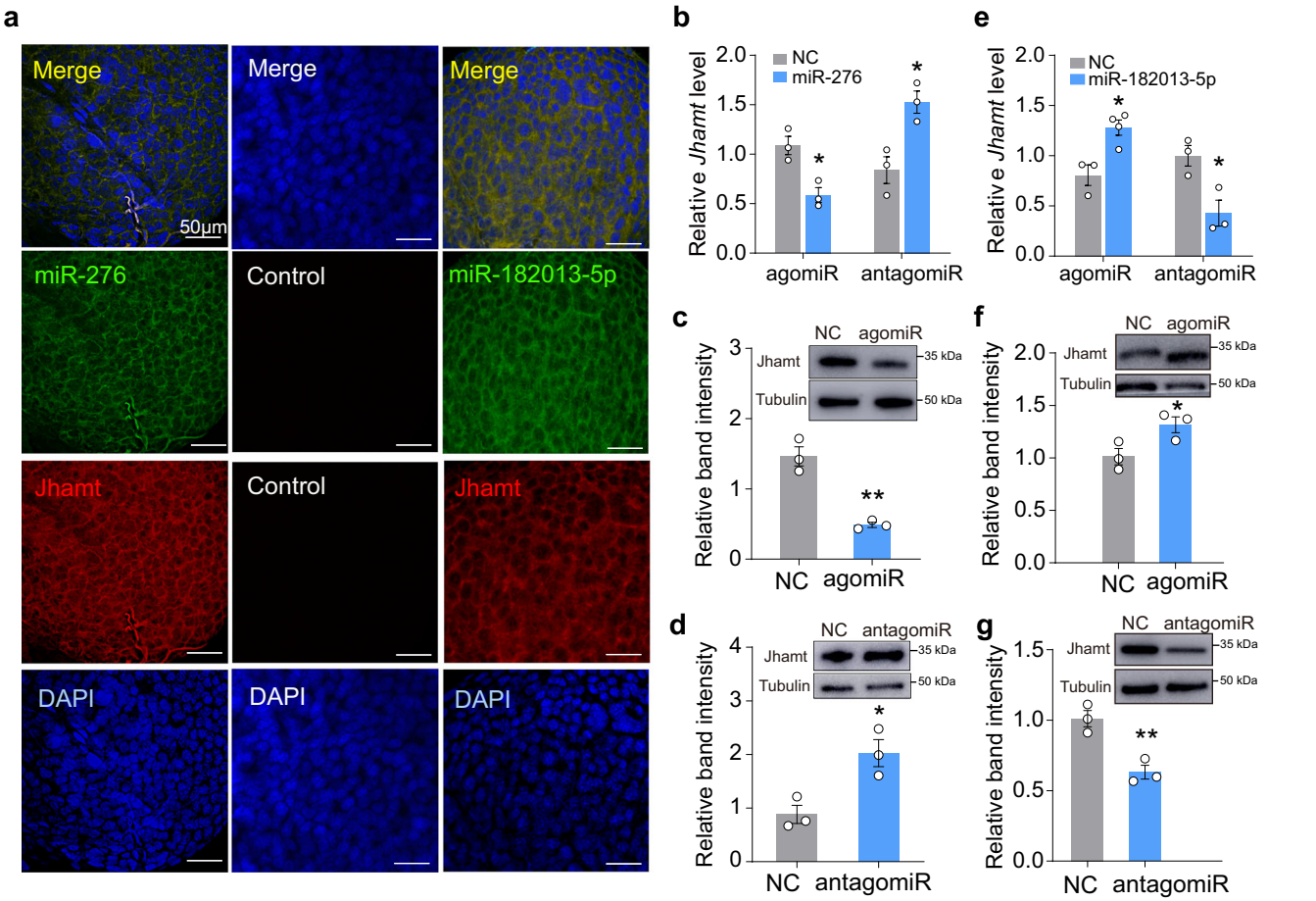

Fig. 3 | Differential regulations of miR-276 and miR-182013-5p in *Jhamt* expression. a Cellular localization of miR-276, miR-182013-5p and *Jhamt* in locust corpora allata (CA). Scale bars, 50 μm. **b** qRT-PCR showing the effect of miR-276 agomiR or antagomiR treatment on *Jhamt* expression in locust CA. NC negative controls. $^{*}P < 0.05$. $n = 6$. **c**, **d** Western blot showing the effect of miR-276 agomiR (**c**) and antagomir (**d**) treatment on *Jhamt* expression in locust CA. $^{*}P < 0.05$; $^{**}P < 0.01$. $n = 3$. **e** Relative mRNA levels of *Jhamt* in the CA of locusts treated with miR-182013-5p agomiR or antagomiR. NC negative controls. $^{*}P < 0.05$. $n = 6$. **f**, **g** Relative protein levels of Jhamt in CA subjected to miR-182013-5p agomiR (**f**) and antagomiR (**g**) treatment. $^{*}P < 0.05$; $^{**}P < 0.01$. $n = 3$.

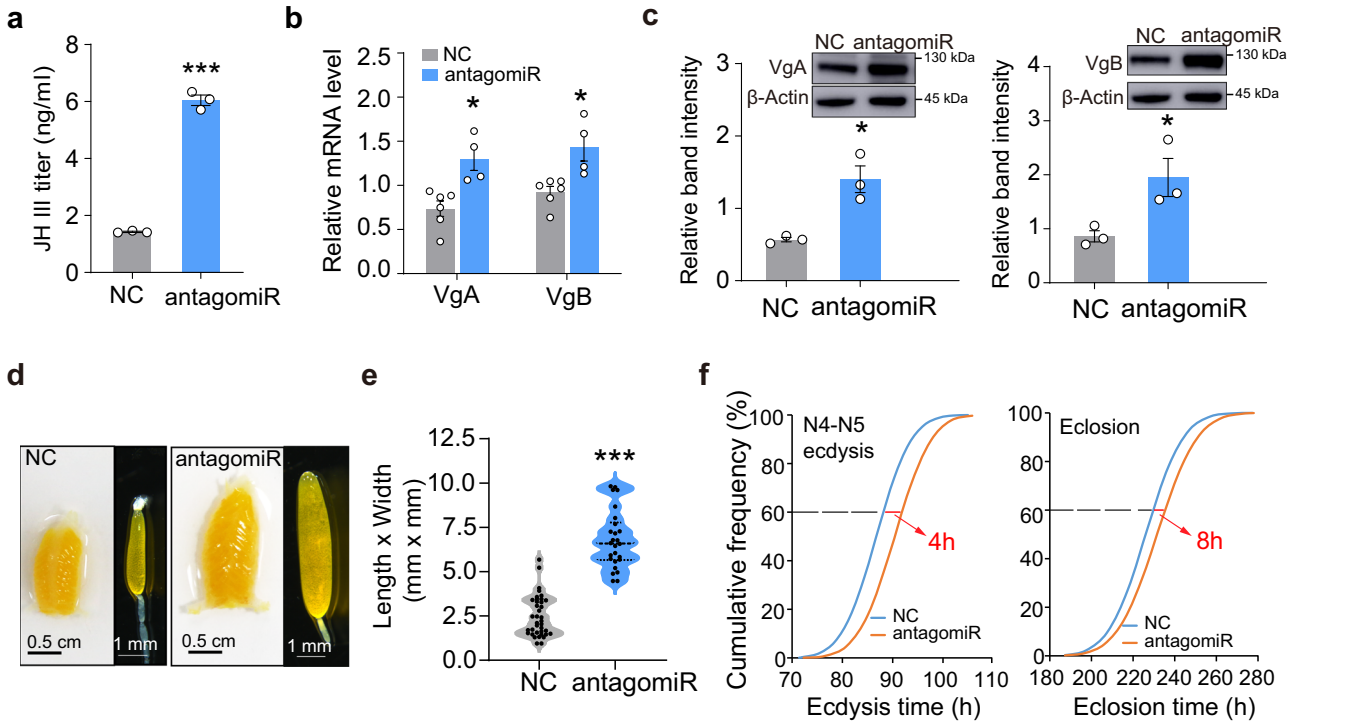

Fig. 4 | Function of miR-276 in locust metamorphosis and female reproduction. **a** Hemolymph JH titers in locusts injected with miR-276 antagomiR or negative control (NC). ***$P < 0.001$. $n = 3$. **b** Effect of miR-276 antagomiR treatment on the mRNA levels of *VgA* and *VgB* in the fat body. *$P < 0.05$. $n = 4–6$. **c** Relative protein levels of VgA and VgB in the fat body of locusts treated with miR-276 antagomir or negative control (NC). *$P < 0.05$. $n = 3$. **d** Representative phenotypes of ovaries and primary oocytes of locusts injected with miR-276 antagomiR or negative control (NC). **e** Statistical analysis of primary oocytes between miR-276 antagomiR or negative control (NC). ***$P < 0.001$. $n = 26–38$. **f** Effect of miR-276 antagomiR treatment on the ecdysis of penultimate 4th (left panel) and final 5th (right panel) instar nymphs. NC negative control; N4, 4th nymph; N5, 5th nymph.

2.5-fold increasement of VgA protein levels and a 2.3-fold elevation of VgB (Fig. 5c). Consistently, miR-276 antagomiR-treated locusts showed accelerate oocyte maturation and ovarian growth (Fig. 4d), with significantly larger primary oocytes (6.80 mm in average) compared to the negative controls (2.48 mm in average) (Fig. 4e). For nymphal locusts, it was found that the period of 4th nymph (N4) was longer than the control group. Statistically, the time of 60% cumulative molting rate of locust treated with antagomiR-276 was 5 h latter than the control (Fig. 4f). This effect was also observed during the nymph-adult transition in the final nymph stage, in which the time of 60% cumulative eclosion rate of antagomiR-276 injected locusts was 8 h later than the control (Fig. 4f).

To comprehensively document the functions of miR-276, agomiR was used to increase its abundance in vivo. As a result of miR-276 agomiR treatment, the expression of *VgA* and *VgB* significantly decreased by 4.2-fold and 2.4-fold (Supplementary Fig. 3a). As shown in Supplementary Fig. 3b, miR-276 agomiR-treated locusts showed retarded oocyte maturation and ovarian growth, with significantly smaller primary oocytes in comparison with the negative controls (Supplementary Fig. 3c). Treatment of miR-276 agomiR also accelerate the development period of 4th nymph by 5 h compared with locust nymphs injected with negative control (Supplementary Fig. 3d). During the nymph-adult eclosion, 60% locusts injected with agomiR eclosed 0.7 h earlier than those of negative control (Supplementary Fig. 3e). Notably, the phenotypes of ovarian growth and nymphal development caused by miR-276 agomiR treatment resembled the effects obtained by *Jhamt* RNAi.

miR-182013-5p promotes JH biosynthesis for locust metamorphosis and female reproduction

Similar with the function studies of miR-276, antagomiR and agomiR were both engaged to illustrate the roles of miR-182013-5p. After injection of miR-182013-5p antagomiR, JH III titer significantly decreased by 3.7-fold of compared with negative control (Fig. 5a). Consequently, the mRNA levels of *VgA* significant reduced by 63.4% and *VgB* significant declined by 50.5% (Fig. 5b). Western blot and band intensity quantification showed that injection of miR-182013-5p antagomiR led to 2.9-fold and 4.4-fold decrease of VgA and VgB protein, respectively (Fig. 5c). As a result, miR-182013-5p antagomiR-treated locusts showed delayed oocyte maturation (Fig. 5d), with significantly smaller oocyte size (Fig. 5e). It was also found that molting time of 60% antagomiR-182013-5p injected locusts was 5 h later than those of treated by negative controls in the 4th nymph stage (Fig. 5f). In the last nymph stage, a 11 h delay in time for 60% locusts to complete the adult eclosion was observed in antagomiR-treated nymphs (Fig. 5f).

Comparatively, in the functional study using agomiR of miR-182013-5p, mRNA levels of *VgA* and *VgB* significantly increased by 2.2-fold and 1.9-fold (Supplementary Fig. 4a). The morphology observation showed that miR-182013-5p agomiR-treated locusts exhibited accelerate oocyte maturation and ovarian growth (Supplementary Fig. 4b), with significantly larger primary oocytes in comparison with the negative controls (Supplementary Fig. 4c). Statistically, for the nymph locusts, 60% locust molted from 4th to 5th nymph delay for 12 h compared with those molted in the negative control (Supplementary Fig. 4d). And a 3 h-delay was observed for 60% locusts eclosed from 5th nymph to the adult (Supplementary Fig. 4d). Taken together, our results suggest that miR-182013-5p play a crucial role in locust molting, metamorphosis and oocyte growth.

miR-276 and miR-182013-5p coordinate *Jhamt* expression during insect metamorphosis and female reproduction

As shown above, miR-276 and miR-182013-5p inversely regulate *Jhamt* level in vivo. We are curious about how miR-276 and miR-182013-5p coordinate to jointly regulate the expression of *Jhamt* and JH production. To

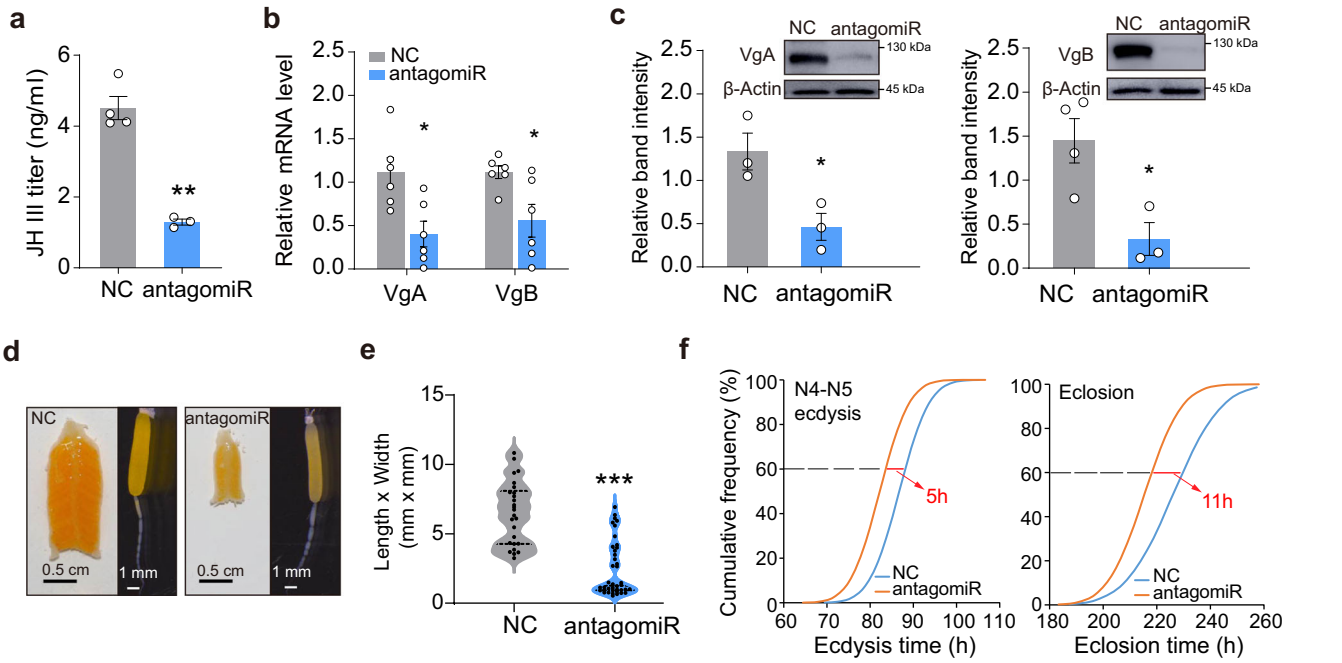

Fig. 5 | Role of miR-182013-5p in locust metamorphosis and female reproduction. a Hemolymph JH titers in locusts injected with miR-182013-5p antagomiR or negative control (NC). $^{**}P < 0.01$. $n = 3$–4. **b** Relative mRNA levels of *VgA* and *VgB* in the fat body of locusts subjected to miR-182013-5p antagomiR treatment. $^{*}P < 0.05$. $n = 6$. **c** Relative protein levels of VgA and VgB in the fat body of locusts treated with miR-182013-5p antagomiR. $^{*}P < 0.05$. $n = 3$–4. **d** Representative phenotypes of ovaries and primary oocytes of locusts treated with miR-182013-5p antagomiR vs. negative control (NC). **e** Statistical analysis of primary oocyte size. $^{***}P < 0.001$. $n = 31$–40. **f** Effect of miR-182013-5p antagomiR treatment on the ecdysis of 4th and 5th instar nymphs. Mann–Whitney *U* test (two-tailed) was applied for two-group comparisons in (**e**).

shed light on this, we first examined and compared their temporal expression patterns. As shown in Fig. 6a, b, the levels of miR-276 peaked during the late N4 and N5 stages compared to the early stages. In contrast to miR-276, the expression of miR-182013-5p peaked in the middle of the N4 stage and sharply declines by late N4. During the 5th nymphal stage, miR-182013-5p maintains an average level lower than that observed in N4. And the pattern was similar with that at N4, although the decline at the late N5 was not statistically significant. While during the adult development, miR-276 levels dropped to the bottom around 4PAE and subsequently rose starting from 5PAE. However, miR-182013-5p slightly increased before 4PAE and dramatically elevated to the top at around 6PAE followed by a significantly decline at 7APE.

Although the expression pattern might partially explain the dynamic actions of miR-276 and miR-182013-5p during the nymphal development. The increase of miR-276 around 5PAE was hard to explain, due to its negative action on Jhamt and JH titer. Given that dynamic miRNA binding to its target is also a critical factor for its functions[41], we developed an in vivo method to quantify dynamic miRNA interactions with *Jhamt*. In brief, freshly dissected CA tissues were crosslinked immediately, *Jhamt*-miRNA complex was immunoprecipitated using a set of biotin-labeled DNA probes against *Jhamt* (Fig. 6c). Total RNAs containing the *Jhamt*-miRNA complex was isolated and the amount of miRNA was determined by qRT-PCR (Fig. 6c). As described in Fig. 6d, at early N4, miR-182013-5p and miR-276 were bound to *Jhamt* in equivalent amounts. However, the amount of *Jhamt*-bound miR-276 significantly declined by 12.8% and 26% in the middle and late stages of N4, respectively, compared with miR-182013-5p. We also compared miRNA bindings in the adult stage. At the pre-vitellogenesis stage, the abundance of *Jhamt*-bound miR-276 at 3PAE and 4PAE was significantly higher than that of miR-182013-5p, by 29.7% and 39.2%, respectively. Intriguingly, during the vitellogenesis stage (5PAE and 6PAE) when JH reaches a high level, Jhamt bound more miR-182013-5p than miR-276 (Fig. 6e). In conclusion, our findings suggest that miR-276 and miR-182013-5p synchronously regulate *Jhamt*, coordinated through their temporal expression patterns and dynamic binding to *Jhamt*.

Discussion

miRNAs targeting *Jhamt* in corpora allata

Jhamt plays a rate-limiting role in JH biosynthesis and regulates JH-related physiology processes such as metamorphosis and vitellogenesis[17,42,43]. Our results showed that knocking down of *Jhamt* leads to significant decrease in hemolymph JH content, Vg production and oocyte growth in migratory locust. Similar effects on insect vitellogenesis and egg production have been reported in other species, including the desert locust *Schistocerca gregaria*[44], the red flour beetle, *T. castaneum*[45] and the colorado potato beetle *Leptinotarsa decemlineata* (Say)[46]. However, the effects such as precocious metamorphosis[47], adult-like deformed organs and increased mortality[48] were not emerged in nymphal locusts after dsJhamt treatment in our current study. We inferenced that the variations in knockdown efficiency may lead to the observed differences in molting and metamorphosis phenotypes. For instance, precocious metamorphosis in silkworms was observed only when *Jhamt* knockdown was achieved using TALEN[47]. Similarly, a study demonstrated the emergence of precocious adults in *T. castaneum* with *Jhamt* RNAi efficiency reaching 95%[49]. Conversely, in nymphal locusts, *Jhamt* expression decreased by only 51.2%, with statistically significant differences. The residual transcripts might still be effective in countering 20E actions during the nymph-adult transition. Nonetheless, a shortened nymphal period, analogous to findings in *L. decemlineata*[46], was documented in locusts depleted of *Jhamt*, consistent with the known function of JH[50].

A previous study in *D. melanogaster* has confirmed that the miRNA bantam is involved in JH synthesis by negatively regulating *Jhamt*. It also provided evidences that *Jhamt* might be regulated by various miRNA families across different insect species, such as *A. gambiae* and *T. castaneum*, as well as in other crustaceans[32]. Overexpression of the bantam microRNA leads to pupal lethality and malformed genitalia in *D. melanogaster*[32]. Our current work has identified two miRNAs that dually regulate *Jhamt* in *L.*

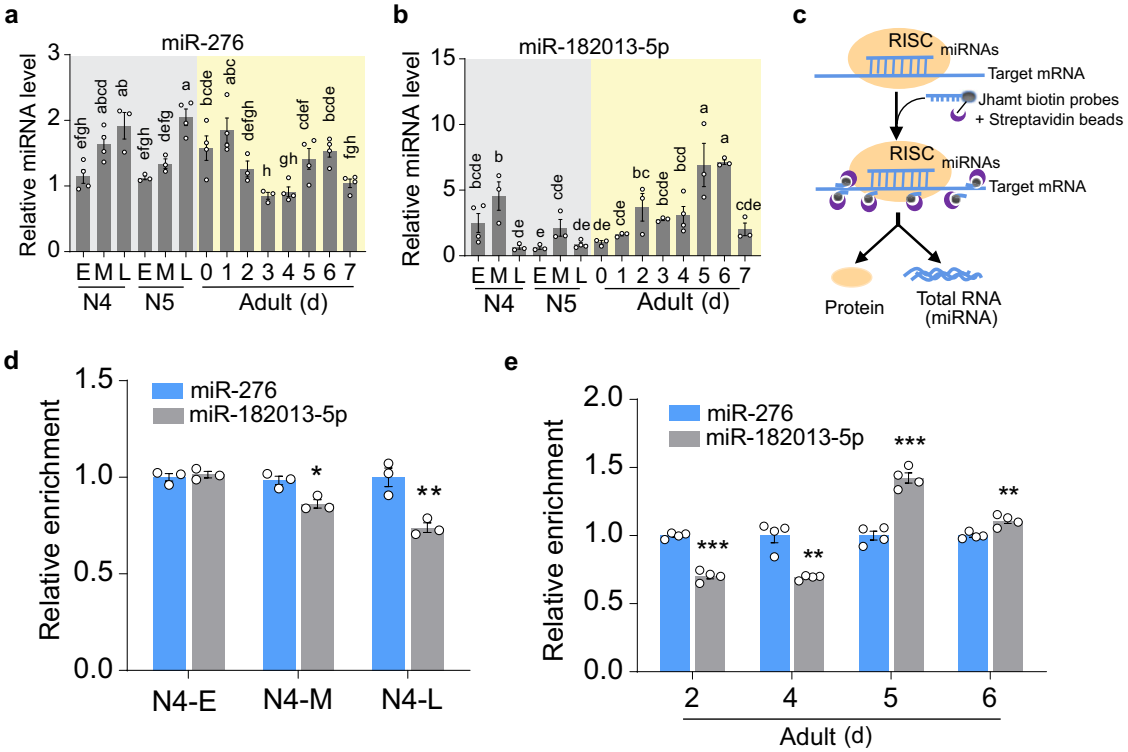

Fig. 6 | Dynamic binding of miR-276 and miR-182013-5p to *Jhamt*. Temporal expression patterns of miR-276 (**a**) and miR-182013-5p (**b**) in the corpus allatum. N4, 4th instar nymphs; N5, 5th instar nymphs; E, early (day 1); M, middle (day 2 for N4, and day 3 for N5); L, late (day 4 for N4, and day 5 for N5). Different letters indicate significant differences at $P < 0.05$. $n = 6$. **c** Diagram illustrating ChIRP procedure for measuring miRNA binding to *Jhamt*. Enrichment of miR-276 and miR-182013-5p from *Jhamt* in the 4th instar nymphal (**d**) and adult (**e**) stages. $^{*}P < 0.05$; $^{**}P < 0.01$; $^{***}P < 0.001$. $n = 3$–4.

migratoria supporting the notion that miRNAs are involved in precisely tuning the developmental JH synthesis. These findings together suggest both a universality and evolutionary significance to the roles of miRNAs in JH biosynthesis[43]. To thoroughly elucidate the functions of miRNAs, we investigated the developmental roles of miR-276 and miR-182013-5p using antagomiR-mediated knockdown and agomiR-mediated overexpression strategies. The changes in JH titers in locusts treated with antagomiRs for miR-276 and miR-182013-5p were distinct, suggesting that they regulate the same target, *Jhamt*, thereby influencing JH titers. Since all phenotypes induced by agomiR treatment were opposite to those observed with antagomiR treatment and closely mirrored JH-related phenotypes[51–53], we conclude that miR-276 and miR-182013 regulate JH production via Jhamt, ultimately modulating metamorphosis and female vitellogenesis.

Moreover, we observed that miR-276 also regulates *Brahma* (*Brm*) in the ovary and plays a role in synchronizing egg hatching in *L. migratoria*[35]. Along with its function in regulating *Jhamt* in CA, these findings are consistent with the understanding that a single miRNA can regulate multiple targets across different tissues or cell types[54–59]. Therefore, our investigations not only demonstrate the involvement of miRNA in regulating *Jhamt* but also expand the understanding of miR-276's functions in *L. migratoria*, highlighting its diverse and significant roles in locusts.

Upregulation of target genes by miRNAs, affecting both protein and mRNA levels, is a non-canonical mechanism that is gradually being uncovered[60–62]. The mechanisms of upregulating protein levels are varied and case-dependent, involving the action of translation activators, the elimination of translation inhibition, and the promotion of nuclear export[35,58,63]. For the regulation at the RNA level, previous studies have elucidated that miRNA can bind to promoters to initiate gene expression[64,65]. In our study, miR-182013-5p was found to upregulate *Jhamt* mRNA levels without enhancing its protein levels. Since miR-182013-5p does not have a binding site in the regulatory promoter regions of Jhamt, we speculate that miR-182013-5p may increase *Jhamt* levels through other pathways. Additionally, the upregulation at the mRNA level may also result from increased mRNA stability, potentially mediated by specific miRNPs (micro-ribonucleoprotein)[59]. We thus speculate that miR-182013-5p may recruit specific miRNPs that could be species- or tissue-specific. In the future, the underlying mechanisms of miR-182013-5p in locust CA will be thoroughly elucidated.

Dual regulation of *Jhamt* by miR-276 and miR-182013-5p

A single miRNA commonly targets multiple genes, and a single gene can be regulated by multiple miRNAs[66–68]. For example, in neural stem cells, miR-124, miR-128, and miR-137 collectively regulate the target gene *Sp1*, orchestrating neural differentiation[69]. In the insect 20E biosynthesis pathway, the halloween gene *Nvd* is co-regulated by two miRNAs, while *Spo* is targeted by seven miRNAs[70]. Using the CLEAR-CLIP method, Fu et al. found that various miRNAs dynamically bound to target genes during different developmental stage, providing new insights into miRNA regulatory actions. Here, we illustrated that miR-276 is a negative regulator while miR-182103 is a positive one of their common target *Jhamt*. While gain and loss of function experiments clearly suggested their involvement in the regulation of *Jhamt*, the nature of their synergistic interaction during locust development remains elusive. The developmental expression profiles of miR-276 indicated that the opposite pattern of miR-276 and *Jhamt* allowed the negative regulator miR-276 to play a positive role during JH synthesis in during gonadotrophic stage. In comparison, the pattern of miR-182013-5p was accordance with *Jhamt*, exserting its function to elevate *Jhamt* abundance and JH synthesis. During the nymphal stage, the concentration of miR-276 sharply increased, peaking just before molting, a period characterized by a significant decrease in JH levels. Conversely, the expression of miR-182013-5p aligned well with the predicted fluctuations of JH titer throughout molting and metamorphosis. To further uncover how they collaborated in regulating *Jhamt*, we adopted and developed the in vivo ChIRP (Chromatin Isolation by RNA Purification) assays for identifying the

dynamic miRNA bindings on a target gene[71,72]. We found that *Jhamt* bound less miR-182013-5p compared to miR-276 when nymphal locusts are about to molt, result in a sharp decrease of JH synthesis to guarantee 20E mediated molting. Intriguingly, in the adult stage, less miR-182013-5p was bond to *Jhamt* compared with miR-276 at the 2 and 4 PAE, whereas at 5 and 6 PAE, *Jhamt* bound more miR-182013-5p than miR-276. We infer that the repressive effects of miRNAs predominate during the pre-vitellogenesis stage, while during vitellogenesis, miRNAs exert a positive influence to ensure robust JH production. Consequently, we proposed that miR-276 and miR-182013-5p, with their opposed regulatory actions, are finely tuned to maintain the requisite JH levels critical for development timing and female reproduction through dynamic interactions with *Jhamt*.

Materials and methods

Insects

The gregarious phase of migratory locust was reared at 30 ± 2 °C and under a photoperiod of 14 h light:10 h dark. The diet included a continuous supply of dry wheat bran with fresh wheat seedlings provided twice daily[39].

Small RNA sequencing and miRNA target prediction

RNAs were extracted from corpora allata (CA). Small RNA sequencing and quantification were performed by Illumina HiSeq 2500 platform. For miRNA analysis, clean reads were obtained by removing the low-quality reads, empty adapters, reads shorter than 18 nt, and reads with Poly(A) tail. Sequences of tRNA, rRNA, snRNA, snoRNA and piRNA were removed by similarity search using the Rfam12.1 and piRNABank database. miRNAs were identified by blasting the rest sequences with miRBase (V22) and referring to the locust genome[73]. To identify conserved miRNAs, we further performed similarity alignment against miRbase (V22). Candidate miRNAs with up to two mismatches to known conserved miRNAs were considered potential locust-specific miRNAs[74,75]. miRNA-binding sites were predicted by miRanda (V3.3a), PITA[76] and MicroTar (V0.9.6), the intersections of results from above three software were selected as candidates.

RNA extraction and qRT-PCR

Total RNA from the selected tissues was isolated using TRNzol reagent (Tiangen). For mRNA quantification, cDNA was reverse transcribed using FastQuant RT Kit (Tiangen). qRT-PCR was performed with SuperReal PreMix Plus kit (Tiangen), began at 95 °C for 2 min, followed by 45 cycles of 95 °C for 20 s, 58 °C for 20 s and 68 °C for 20 s. Primers used for mRNA qRT-PCR were listed in Table S1. For miRNA verification, cDNA was prepared with the miRNA first strand cDNA synthesis kit (Tiangen). qRT-PCR of miRNA was performed using the miRcute miRNA qPCR kit (Tiangen) at 94 °C for 2 min plus 40 cycles of 94 °C for 20 s and 60 °C for 34 s. Primers used for qRT-PCR of miRNA were listed in Table S2. The relative expression was calculated with the $2^{-\Delta\Delta Ct}$ method, U6 and β-actin were used as the internal controls for mRNA and miRNA, respectively.

Luciferase reporter assay

The luciferase reporter assay was performed as described in previous studies[39,77]. In detail, *Jhamt* fragments with miRNA-binding sites were cloned into pmirGLO vector (Promega) for dual-luciferase reporter experiments. For site mutation, the miRNA seed regions were mutated to complementary sequences using Site-directed and Ligase-Independent Mutagenesis[78]. To minimize potential interference from endogenous miRNAs, HEK293T cells were selected for the luciferase assay. Commercial synthesized miRNA mimics (GenePharma, Shanghai) were used for miRNA overexpression in the HEK293T cells. The negative control of miRNA mimics was a random sequence according to *Caenorhabditis elegans* miRNAs. Mimics of miR-182013-5p and miR-276, as well as the negative control, were respectively co-transfected with the recombinant pmirGLO/*Jhamt* vector into HEK293T cells utilizing Lipofectamine 3000 (Thermo Fisher). After 36 h, the luciferase activity was measured using the Dual-Glo Luciferase Assay System (Promega) and GloMax 96 Microplate Luminometer (Promega).

RNA interference, agomiR and antagomiR treatment

For RNAi experiments, dsRNA of *Jhamt* and green fluorescent protein (GFP) were synthesized using T7 RiboMAX Express RNAi system (Promega). The primers used for dsRNA synthesis are listed in Table S3. The adult females were intra-abdominally injected with 15 μg dsRNA within 12 h of adult emergence and an additional dose on day 5. For nymphal locusts, 4th instar nymphs within 24 h of molting were injected with 7 μg dsRNA. In the agomiR and antagomiR treatment, adult locusts within 12 h after eclosion were injected with miRNA agomiR or antagomiR (GenePharma) at dose of 1 nmol mixed with in vivo RNA Transfection Reagent (Engreen), and boosted twice on day 3 and day 6. For the treatment in nymphal locusts, 0.5 nmol agomiR or antagomiR were injected into the 4th instar nymphs within 1 h of molting. A subsequent injection was given at the first day of 5th instar, with an additional booster on day 3 of the 5th instar. A nucleotide sequence from *C. elegans* genome (sense: 5′-UUCUCCGAACGUGUCACGUTT-3′; antisense: 5′-ACGUGACACGUUCGGAGA-ATT-3′) was served as the negative control in agomiR or antagomiR treatment.

Jhamt antibody preparation

A 252-bp cDNA fragment coding for an 84-aa peptide (forward primer: 5′-TTCTCCTTCTTCTGCCTTC-3′; reverse primer: 5′-CGGATCTC-CATCGTGTCC-3′) of locust Jhamt was cloned into pET-32a-His and confirmed by sequencing. The recombinant Jhamt peptide was purified using an NTA-Ni2+-affinity column (CWBIO) and analyzed by SDS-PAGE. Polyclonal antibodies against Jhamt were generated in rabbits through immunization with the recombinant peptide emulsified with Freund's complete adjuvant (Sigma-Aldrich). New Zealand White rabbits (*Oryctolagus cuniculus*) were injected subcutaneously at four sites and received weekly boosts for a total of five injections. Given that Jhamt is exclusively expressed in corpora allata, the specificity of the antiserum was confirmed by western blot using protein extracts from both the fat body and corpora allata (Supplementary Fig. 5). We have adhered to all relevant ethical guidelines regarding the use of animals.

Western blot

Total proteins were extracted from the corpora allata or the fat body using lysis buffer containing 50 mM Tris-HCl (pH 7.5), 150 mM NaCl, 2 mM EDTA, 1 mM DTT, 1% Triton X-100 and a protease inhibitor cocktail (Roche). The tissue lysates were then cleared by centrifugation at 12,000 g at 4 °C for 30 min. Extracted proteins were quantified using a BCA protein assay kit (Pierce), fractionated on 8% SDS-PAGE, and then transferred to PVDF membranes (Millipore). Western blot was carried out using antiserums against locust Jhamt (1:5000), VgA (1:5000) and VgB (1:5000). β-actin (BM5422, BOSTER, 1:10,000) and β-Tubulin (A05397-1, BOSTER, 1:10,000) was used as a loading control. Bands were imaged with Amersham Imager 600 (GE Healthcare) and analyzed using ImageJ software.

Fish

The RNA probes for in situ hybridization were designed and commercial synthesized (GenePharma, Shanghai). They were selected for the highest specificity after alignment with genome and transcriptome, the sequences of probes were listed in Table S4. *Jhamt* probes were tagged with CY3 for red fluorescence, and miRNA-specific probes with FAM for green fluorescence. For tissue preparation and fixation, freshly dissected CA tissues from were fixed in a 4% paraformaldehyde solution at room temperature, followed by incubation with 0.1% Triton X-100. The tissues were then washed twice using PBS and pre-incubated in 2× SSC at 37 °C. RNA probes were diluted in hybridization buffer to a final concentration of 1 μM. Hybridization was performed at 73 °C for 5 min, subsequent to which the probe was applied to the tissues for an overnight incubation at 37 °C in a rotating chamber shielded from light. The following day comprised a sequence of washes in a wash buffer containing 0.1% Tween-20 and 99.9% 4× SSC at 42 °C, followed by additional washes in 2× and 1× SSC solutions. Subsequently, tissues were

stained with Hoechst solution and subjected to two washes with PBS. The tissue was imaged using laser scanning confocal microscopes (N-SIM/A1, Nikon).

Optimized chromatin isolation by RNA purification (ChIRP)

DNA probes were designed using online resources (https://www.biosearchtech.com) following specific criteria[71]. Totally, 10 probes against the full-length mRNA of *Jhamt* was designed, and probes of LacZ were used as controls. Freshly dissected CA tissues from 30-50 individual locusts were mixed and cooled on ice. The chromatin isolation was conducted using the ChIRP kit (SCBIO). In brief, samples were centrifuged at 800 rcf for 4 min at 25 °C to collect tissues. The tissue pellet was then incubated in 2% paraformaldehyde solution at room temperature for 10 min. Afterward, 100 µl of 1.25 M glycine solution was added, and the mixture was incubated at room temperature for 5 min for reverse crosslinking. The tissue suspension was then centrifuged at 2000 rcf for 5 min at room temperature, and the supernatant was discarded. The tissues were washed with PBS and centrifuged at 2000 rcf for 5 min at 4 °C to remove any remaining supernatant. Lysis Buffer (containing 12 µL PMSF, 10 µL proteinase inhibitor, and 5 µL RNase inhibitor) was added to lyse the CA tissues, and the mixture was gently shaken in a 30-minute ice bath. A 50 µL aliquot was collected from the lysate as Input. Hybridization Buffer, with twice the volume of the remaining lysate, was added to the tissue lysate, and then probes were added to achieve a final concentration of 0.5 ng/ml. The mixtures were incubated at 37 °C with rotation for 4 h. After incubation, pre-washed streptavidin magnetic beads were added to the mixture and incubated at 37 °C with rotation for 30 min. Following incubation, the supernatant was removed, and the beads were washed with Wash Buffer at 37 °C with rotation for 5 min, repeating this wash process five times. Finally, the magnetic beads were used for RNA extraction

Statistics and reproducibility

To detect mRNA and miRNA levels in the CA, 2–4 locusts were collected and pooled as a single biological replicate. For all other tissue types, excluding the CA, one biological replicate consisted of a single individual locust. All the measurements were taken from distinct samples.

For two-group comparisons, normality was assessed using the Kolmogorov-Smirnov test. Two-tailed student's t-test was applied for data with normal distribution, while the Mann–Whitney *U* test (two-tailed) was used for non-normal distributions. When the Mann–Whitney *U* test was used, it was explicitly noted in the figure legend. Unless otherwise stated, Student's t-test was used to assess significance in two-group comparisons. Multiple comparisons were conducted using one-way ANOVA followed by LSD (least significant difference) post-hoc adjustment. Additional details on statistical analyses, sample sizes, and biological replicates are provided in the figure legends.

All statistical analyses were performed in Prism 9. Values are shown as mean ± s.e.m. and significant difference was considered at $P < 0.05$. Source data of the figures were attached in the supplementary files. Heatmap was generated using pheatmap package (v2.20.0) in R (v4.4.1). Other graphs were prepared using Prism GraphPad 9 and Adobe Illustrator 2021.

Reporting summary

Further information on research design is available in the Nature Portfolio Reporting Summary linked to this article.

Data availability

The raw data for miRNA transcriptome have been deposited at NCBI (PRJNA1181594). All the data are available in the article and Supplementary files. Source data are provided in this paper in Supplementary Data 1. Uncropped western blots are found in Supplementary data 2. Any remaining information can be obtained from the corresponding author upon reasonable request.

Received: 1 August 2024; Accepted: 18 November 2024;
Published online: 02 December 2024

References

1. Wu, Z., Yang, L., He, Q. & Zhou, S. Regulatory mechanisms of vitellogenesis in insects. *Front. Cell Dev. Biol*. **8**, https://doi.org/10.3389/fcell.2020.593613 (2021).
2. Jindra, M., Palli, S. R. & Riddiford, L. M. The juvenile hormone signaling pathway in insect development. *Annu. Rev. Entomol.* **58**, 181–204 (2013).
3. Roy, S., Saha, T. T., Zou, Z. & Raikhel, A. S. Regulatory pathways controlling female insect reproduction. *Annu. Rev. Entomol.* **63**, 489–511 (2018).
4. Riddiford, L. M. Cellular and molecular actions of juvenile hormone I. General considerations and premetamorphic actions. *Adv. Insect Phys.* **24**, 213–274 (1994).
5. Raikhel, A. S., Brown, M. R. & Belles, X. in *Comprehensive Molecular Insect Science* (ed Gilbert, L. I.) 433–491 (Elsevier, 2005).
6. Truman, J. W. & Riddiford, L. M. The evolution of insect metamorphosis: a developmental and endocrine view. *Philos. T R. Soc. B* **374**, 20190070 (2019).
7. Truman, J. W. & Riddiford, L. M. The origins of insect metamorphosis. *Nature* **401**, 447–452 (1999).
8. Cruz, J. et al. Quantity does matter. Juvenile hormone and the onset of vitellogenesis in the German cockroach. *Insect Biochem. Mol. Biol.* **33**, 1219–1225 (2003).
9. Marchal, E., Hult, E. F., Huang, J., Stay, B. & Tobe, S. S. Diploptera punctata as a model for studying the endocrinology of arthropod reproduction and development. *Gen. Comp. Endocrinol.* **188**, 85–93 (2013).
10. Guo, W. et al. Juvenile hormone-dependent Kazal-type serine protease inhibitor Greglin safeguards insect vitellogenesis and egg production. *FASEB J.* **33**, 917–927 (2019).
11. Leyria, J. Endocrine factors modulating vitellogenesis and oogenesis in insects: an update. *Mol. Cell Endocrinol.* **587**, 112211 (2024).
12. Dubrovsky, E. B. Hormonal cross talk in insect development. *Trends Endocrinol. Metab.* **16**, 6–11 (2005).
13. Huang, J., Marchal, E., Hult, E. F. & Tobe, S. S. Characterization of the juvenile hormone pathway in the viviparous cockroach, *Diploptera punctata*. *PLoS ONE* **10**, e0117291 (2015).
14. Belles, X., Martin, D. & Piulachs, M. D. The mevalonate pathway and the synthesis of juvenile hormone in insects. *Annu Rev. Entomol.* **50**, 181–199 (2005).
15. Defelipe, L. A. et al. Juvenile hormone synthesis: "esterify then epoxidize" or "epoxidize then esterify"? Insights from the structural characterization of juvenile hormone acid methyltransferase. *Insect Biochem. Mol. Biol.* **41**, 228–235 (2011).
16. Kort, C. A. D. & Granger, N. A. Regulation of the juvenile hormone titer. *Annu. Rev. Entomol.* **26**, 1–28 (1981).
17. Shinoda, T. & Itoyama, K. Juvenile hormone acid methyltransferase: a key regulatory enzyme for insect metamorphosis. *Proc. Natl Acad. Sci. USA* **100**, 11986–11991 (2003).
18. Sakurai, S. & Niimi, S. Development changes in juvenile hormone and juvenile hormone acid titers in the hemolymph and in-vitro juvenile hormone synthesis by corpora allata of the silkworm, *Bombyx mori*. *J. Insect Physiol.* **43**, 875–884 (1997).
19. Zhou, C. et al. Role of SfJHAMT and SfFAMeT in the reproductive regulation of *Sogatella furcifera* and its expression under insecticide stress. *Pestic. Biochem. Physiol.* **173**, 104779 (2021).
20. Dominguez, C. V. & Maestro, J. L. Expression of juvenile hormone acid O-methyltransferase and juvenile hormone synthesis in *Blattella germanica*. *Insect Sci*. https://doi.org/10.1111/1744-7917.12467 (2017).
21. Liu, S. et al. Antagonistic actions of juvenile hormone and 20-hydroxyecdysone within the ring gland determine developmental

transitions in Drosophila. *Proc. Natl Acad. Sci. USA* **115**, 139–144 (2018).
22. Huang, J. et al. DPP-mediated TGFbeta signaling regulates juvenile hormone biosynthesis by activating the expression of juvenile hormone acid methyltransferase. *Development* **138**, 2283–2291 (2011).
23. Ishimaru, Y. et al. TGF-beta signaling in insects regulates metamorphosis via juvenile hormone biosynthesis. *Proc. Natl Acad. Sci. USA* **113**, 5634–5639 (2016).
24. Cai, R. et al. POU-M2 promotes juvenile hormone biosynthesis by directly activating the transcription of juvenile hormone synthetic enzyme genes in *Bombyx mori*. *Open Biol.* **12**, 220031 (2022).
25. Meng, M. et al. Homeodomain protein Scr regulates the transcription of genes involved in juvenile hormone biosynthesis in the silkworm. *Int. J. Mol. Sci.* **16**, 26166–26185 (2015).
26. Pasquinelli, A. E. MicroRNAs and their targets: recognition, regulation and an emerging reciprocal relationship. *Nat. Rev. Genet.* **13**, 271–282 (2012).
27. Song, J. & Zhou, S. Post-transcriptional regulation of insect metamorphosis and oogenesis. *Cell Mol. Life Sci.* **77**, 1893–1909 (2020).
28. Li, C. et al. miRNA-mediated interactions in and between plants and insects. *Int. J. Mol. Sci*. **19**, https://doi.org/10.3390/ijms19103239 (2018).
29. Belles, X. MicroRNAs and the Evolution of Insect Metamorphosis. *Annu. Rev. Entomol*. **62**, 111–125 (2017).
30. Zhang, Q., Dou, W., Taning, C. N. T., Smagghe, G. & Wang, J. J. Regulatory roles of microRNAs in insect pests: prospective targets for insect pest control. *Curr. Opin. Biotechnol.* **70**, 158–166 (2021).
31. Asgari, S. MicroRNA functions in insects. *Insect Biochem. Mol. Biol.* **43**, 388–397 (2013).
32. Qu, Z. et al. MicroRNAs regulate the sesquiterpenoid hormonal pathway in Drosophila and other arthropods. *Proc. Biol. Sci.* **284**, https://doi.org/10.1098/rspb.2017.1827 (2017).
33. Zhang, J. et al. MicroRNA miR-8 promotes cell growth of corpus allatum and juvenile hormone biosynthesis independent of insulin/IGF signaling in *Drosophila melanogaster*. *Insect Biochem. Mol. Biol.* **136**, 11 (2021).
34. Lee, S. et al. Ecdysone-induced microRNA miR-276a-3p controls developmental growth by targeting the insulin-like receptor in Drosophila. *Insect Mol. Biol.* **32**, 703–715 (2023).
35. He, J. et al. MicroRNA-276 promotes egg-hatching synchrony by up-regulating brm in locusts. *Proc. Natl Acad. Sci. USA* **113**, 584–589 (2016).
36. Chen, X. & Rosbash, M. mir-276a strengthens Drosophila circadian rhythms by regulating timeless expression. *Proc. Natl Acad. Sci. USA* **113**, E2965–E2972 (2016).
37. Li, W. et al. MicroRNA-276a functions in ellipsoid body and mushroom body neurons for naive and conditioned olfactory avoidance in drosophila. *J. Neurosci.* **33**, 5821–5833 (2013).
38. Li, H. & Gavis, E. R. Drosophila FMRP controls miR-276-mediated regulation of nejire mRNA for space-filling dendrite development. *G3 (Bethesda)* **12**, https://doi.org/10.1093/g3journal/jkac239 (2022).
39. Song, J. et al. The microRNAs let-7 and miR-278 regulate insect metamorphosis and oogenesis by targeting the juvenile hormone early-response gene Kruppel-homolog 1. *Development* **145**, https://doi.org/10.1242/dev.170670 (2018).
40. Li, W. et al. The miRNA-mRNA modules enhance juvenile hormone biosynthesis for insect vitellogenesis and egg production. *Insect Sci*. https://doi.org/10.1111/1744-7917.13451 (2024).
41. Fu, X., Liu, P., Dimopoulos, G. & Zhu, J. Dynamic miRNA-mRNA interactions coordinate gene expression in adult *Anopheles gambiae*. *PLoS Genet* **16**, e1008765 (2020).
42. Li, K., Jia, Q. Q. & Li, S. Juvenile hormone signaling - a mini review. *Insect Sci.* **26**, 600–606 (2019).
43. Qu, Z., Bendena, W. G., Tobe, S. S. & Hui, J. H. L. Juvenile hormone and sesquiterpenoids in arthropods: Biosynthesis, signaling, and role of MicroRNA. *J. Steroid Biochem Mol. Biol.* https://doi.org/10.1016/j.jsbmb.2018.01.013 (2018).
44. Marchal, E. et al. Final steps in juvenile hormone biosynthesis in the desert locust, *Schistocerca gregaria*. *Insect Biochem Mol. Biol.* **41**, 219–227 (2011).
45. Sheng, Z. T., Xu, J. J., Bai, H., Zhu, F. & Palli, S. R. Juvenile hormone regulates vitellogenin gene expression through Insulin-like Peptide Signaling Pathway in the Red Flour Beetle, *Tribolium castaneum*. *J. Biol. Chem.* **286**, 41924–41936 (2011).
46. Fu, K. Y. et al. Knockdown of juvenile hormone acid methyl transferase severely affects the performance of *Leptinotarsa decemlineata* (Say) larvae and adults. *Pest Manag. Sci.* **72**, 1231–1241 (2016).
47. Daimon, T., Uchibori, M., Nakao, H., Sezutsu, H. & Shinoda, T. Knockout silkworms reveal a dispensable role for juvenile hormones in holometabolous life cycle. *Proc. Natl Acad. Sci. USA* **112**, E4226–E4235 (2015).
48. Niwa, R. et al. Juvenile hormone acid O-methyltransferase in Drosophila melanogaster. *Insect Biochem. Mol. Biol.* **38**, 714–720 (2008).
49. Minakuchi, C., Namiki, T., Yoshiyama, M. & Shinoda, T. RNAi-mediated knockdown of juvenile hormone acid O-methyltransferase gene causes precocious metamorphosis in the red flour beetle *Tribolium castaneum*. *FEBS J.* **275**, 2919–2931 (2008).
50. Riddiford, L. M. Juvenile hormone: the status of its "status quo" action. *Arch. Insect Biochem. Physiol.* **32**, 271–286 (1996).
51. Song, J., Wu, Z., Wang, Z., Deng, S. & Zhou, S. Kruppel-homolog 1 mediates juvenile hormone action to promote vitellogenesis and oocyte maturation in the migratory locust. *Insect Biochem. Mol. Biol.* **52**, 94–101 (2014).
52. Guo, W. et al. Juvenile hormone-receptor complex acts on *mcm4* and *mcm7* to promote polyploidy and vitellogenesis in the *migratory locust*. *PLoS Genet.* **10**, e1004702 (2014).
53. Wu, Z., Yang, L., Li, H. & Zhou, S. Krüppel-homolog 1 exerts anti-metamorphic and vitellogenic functions in insects via phosphorylation-mediated recruitment of specific cofactors. *BMC Biol.* **19**, 222–222 (2021).
54. Hashimoto, Y., Akiyama, Y. & Yuasa, Y. Multiple-to-multiple relationships between microRNAs and target genes in gastric cancer. *PLoS ONE* **8**, e62589 (2013).
55. Nam, J.-W. et al. Global analyses of the effect of different cellular contexts on microRNA targeting. *Mol. Cell* **53**, 1031–1043 (2014).
56. Cordes, K. R. et al. miR-145 and miR-143 regulate smooth muscle cell fate and plasticity. *Nature* **460**, 705–710 (2009).
57. Li, E., Zhang, J., Yuan, T. & Ma, B. MiR-145 inhibits osteosarcoma cells proliferation and invasion by targeting ROCK1. *Tumour Biol.* **35**, 7645–7650 (2014).
58. Vasudevan, S., Tong, Y. & Steitz, J. A. Switching from repression to activation: microRNAs can up-regulate translation. *Science* **318**, 1931–1934 (2007).
59. Valinezhad Orang, A., Safaralizadeh, R. & Kazemzadeh-Bavili, M. Mechanisms of miRNA-mediated gene regulation from common downregulation to mRNA-specific upregulation. *Int. J. Genomics* **2014**, 970607 (2014).
60. Liu, H. et al. Nuclear functions of mammalian MicroRNAs in gene regulation, immunity and cancer. *Mol. Cancer* **17**, 64 (2018).
61. Janowski, B. A. et al. Activating gene expression in mammalian cells with promoter-targeted duplex RNAs. *Nat. Chem. Biol.* **3**, 166–173 (2007).
62. Li, L. C. et al. Small dsRNAs induce transcriptional activation in human cells. *Proc. Natl Acad. Sci. USA* **103**, 17337–17342 (2006).
63. Eiring, A. M. et al. miR-328 functions as an RNA decoy to modulate hnRNP E2 regulation of mRNA translation in leukemic blasts. *Cell* **140**, 652–665 (2010).

64. Xiao, M. et al. MicroRNAs activate gene transcription epigenetically as an enhancer trigger. *RNA Biol.* **14**, 1326–1334 (2017).
65. Place, R. F., Li, L. C., Pookot, D., Noonan, E. J. & Dahiya, R. MicroRNA-373 induces expression of genes with complementary promoter sequences. *Proc. Natl Acad. Sci. USA* **105**, 1608–1613 (2008).
66. Pu, M. et al. Regulatory network of miRNA on its target: coordination between transcriptional and post-transcriptional regulation of gene expression. *Cell Mol. Life Sci.* **76**, 441–451 (2019).
67. Peter, M. E. Targeting of mRNAs by multiple miRNAs: the next step. *Oncogene* **29**, 2161–2164 (2010).
68. Enright, A. J. et al. MicroRNA targets in Drosophila. *Genome Biol.* **5**, R1 (2003).
69. Santos, M. C. et al. miR-124, -128, and -137 orchestrate neural differentiation by acting on overlapping gene sets containing a highly connected transcription factor network. *Stem Cells* **34**, 220–232 (2016).
70. He, K. et al. Multiple miRNAs jointly regulate the biosynthesis of ecdysteroid in the holometabolous insects, Chilo suppressalis. *RNA* **23**, 1817–1833 (2017).
71. Chu, C. et al. Systematic discovery of Xist RNA binding proteins. *Cell* **161**, 404–416 (2015).
72. Chu, C., Qu, K., Zhong, F. L., Artandi, S. E. & Chang, H. Y. Genomic maps of long noncoding RNA occupancy reveal principles of RNA-chromatin interactions. *Mol. Cell* **44**, 667–678 (2011).
73. Wang, X. et al. The locust genome provides insight into swarm formation and long-distance flight. *Nat. Commun.* **5**, 2957 (2014).
74. Wei, Y. Y., Chen, S., Yang, P. C., Ma, Z. Y. & Kang, L. Characterization and comparative profiling of the small RNA transcriptomes in two phases of locust. *Genome Biol* **10**, https://doi.org/10.1186/gb-2009-10-1-r6 (2009).
75. Song, J., Guo, W., Jiang, F., Kang, L. & Zhou, S. Argonaute 1 is indispensable for juvenile hormone mediated oogenesis in the migratory locust, Locusta migratoria. *Insect Biochem. Mol. Biol.* **43**, 879–887 (2013).
76. Kertesz, M., Iovino, N., Unnerstall, U., Gaul, U. & Segal, E. The role of site accessibility in microRNA target recognition. *Nat. Rev. Genet.* **39**, 1278–1284 (2007).
77. Song, J., Li, W., Zhao, H. & Zhou, S. Clustered miR-2, miR-13a, miR-13b and miR-71 coordinately target Notch gene to regulate oogenesis of the migratory locust Locusta migratoria. *Insect Biochem. Mol. Biol.* **106**, 39–46 (2019).
78. Chiu, J., March, P. E., Lee, R. & Tillett, D. Site-directed, ligase-independent mutagenesis (SLIM): a single-tube methodology approaching 100% efficiency in 4 h. *Nucleic Acids Res.* **32**, https://doi.org/10.1093/nar/gnh172 (2004).

Acknowledgements

This work was supported by National Key R&D Program of China 2022YFD1400500, the Outstanding Youth Foundation of Henan Province 202300410040, National Natural Science Foundation of China grants 32070489 and 31702063, Key R&D Program of Henan Province 221111112200, and Natural Science Foundation of Henan Province 232300420185.

Author contributions

J.S., W.L., and S.Z. designed the project; W.L., J.S., L.G., Q.Y., X.Z., and M.L. performed research; J.S. and W.L. analyzed data; J.S., W.L., and S.Z. wrote the paper.

Ethics statement

The procedures for care and use of animals were approved by the Ethics Committee of Henan University.

Competing interests

The authors declare no competing interests.

Additional information

Supplementary information The online version contains supplementary material available at https://doi.org/10.1038/s42003-024-07285-0.

Correspondence and requests for materials should be addressed to Shutang Zhou.

Peer review information *Communications Biology* thanks the anonymous reviewers for their contribution to the peer review of this work. Primary Handling Editors: Jun Wei Pek and Kaliya Georgieva.